

This document is confidential and is proprietary to the American Chemical Society and its authors. Do not copy or disclose without written permission. If you have received this item in error, notify the sender and delete all copies.

Unusual Transformation of Mixed Isomer Decahydroisoquinoline Stable Glasses

Journal:	<i>The Journal of Physical Chemistry</i>
Manuscript ID	jp-2023-00459s.R2
Manuscript Type:	Special Issue Article
Date Submitted by the Author:	06-Jun-2023
Complete List of Authors:	Kasting, Benjamin; University of Wisconsin-Madison, Chemistry Gabriel, Jan; Arizona State University Tracy, Megan; University of Wisconsin Madison, Chemistry Guiseppi-Elie, Anthony; Texas A&M Engineering, Biomedical Engineering Richert, Ranko; Arizona State University Ediger, Mark; University of Wisconsin Madison, Chemistry

SCHOLARONE™
Manuscripts

Unusual transformation of mixed isomer decahydroisoquinoline stable glasses

B.J. Kasting¹, J.P. Gabriel², M.E. Tracy¹, A. Guiseppi-Elie³, R. Richert², M.D. Ediger^{1*}

¹ Department of Chemistry, University of Wisconsin-Madison, Madison, Wisconsin 53706, USA

² Department of Chemistry and Biochemistry, Arizona State University, Tempe, Arizona 85287, USA

³ Department of Biomedical Engineering, College of Engineering, Texas A&M University, College Station, Texas 77843, USA

*Corresponding Author: ediger@chem.wisc.edu

Abstract

Dielectric relaxation was used to characterize the ability of vapor-deposited mixtures of *cis*- and *trans*-decahydroisoquinoline (DHIQ) to form glasses with high kinetic stability. Vapor-deposited mixtures are technologically relevant, and the effect of mixing on glass stability is a relatively unexplored area. Mixed isomers and pure *trans*-DHIQ form highly stable glasses that isothermally transform in approximately $10^4 \tau_a$ (where τ_a is the structural relaxation time of the supercooled liquid). Isomeric composition of the glasses does not play a significant role in the maximum kinetic stability of the resulting films. Secondary relaxations in DHIQ are associated with an intramolecular conformation change and are suppressed to a significant extent in highly stable glasses. During isothermal annealing experiments, stable glasses were found to transform initially via a growth front mechanism which transitions to a homogeneous bulk mechanism. Surprisingly, the time dependence of the bulk transformation is different than reported for other stable glasses and cannot be interpreted in terms of a simple nucleation and growth model.

Introduction

Glasses are fascinating nonequilibrium amorphous materials that play a critical role in modern technology and also pose important conceptual challenges.¹⁻³ In addition to the silicate glasses used for windows and packaging, polymer glasses are utilized at a massive scale. Glasses

1
2
3
4
5
6
7
8
9
10
11
12
13
14
15
16
17
18
19
20
21
22
23
24
25
26
27
28
29
30
31
32
33
34
35
36
37
38
39
40
41
42
43
44
45
46
47
48
49
50
51
52
53
54
55
56
57
58
59
60
are also critical for modern communications in optical fibers and organic light emitting diodes (OLEDs). On the fundamental side, much recent work has focused on the supercooled liquid from which glasses are typically produced, exploring locally-favored structures in the supercooled liquid,⁴⁻⁶ the existence of multiple liquid states⁷⁻⁹, even for single component systems, and the possibility of a thermodynamic transition underlying the laboratory glass transition.^{2, 10} As non-equilibrium materials, how glasses are prepared plays a critical role in determining their properties, and any factors that influence the structure of the supercooled liquid can also have an impact on the structure of a glass.

Physical vapor deposition (PVD) is a well-established technique to prepare glassy thin films of a wide array of materials including small organic molecules¹¹⁻¹⁴, chalcogenides¹⁵⁻¹⁶, metallic glasses¹⁷⁻¹⁸, and polymers.¹⁹⁻²¹ Glasses produced via PVD can have remarkable properties that cannot be achieved using other preparation techniques, including reduced enthalpy^{12, 22-24}, increased density^{20, 25-28}, multiple amorphous structures²⁹, suppressed secondary relaxations³⁰⁻³², and anisotropic molecular orientation³³⁻³⁴. In addition, PVD glasses can exhibit high kinetic stability, which is the tendency to resist devitrification upon heating a glass above its glass transition temperature, T_g . Significant progress has been made to understand how deposition conditions and molecular shape³⁵⁻³⁶ control the structure and properties of the resulting glass. With a few exceptions³⁷⁻³⁹, this fundamental work has been done on single component systems.

Understanding the properties of PVD glasses with more than one component is an important goal for both fundamental and practical reasons. On the application side, the commercial dominance of organic light emitting diode (OLED) displays in the mobile device industry demonstrates the economic importance of vapor-deposited organic glasses.⁴⁰ The active layers in OLEDs are vapor-deposited glasses of organic semiconductors, and often these layers contain

more than one component, e.g., the emitter molecules are usually co-deposited with a host material.⁴¹⁻⁴² The effect of mixing on the kinetic stability of vapor-deposited glasses has been previously studied. In one example, a low concentration (~5%) of 4,4'-diphenyl azobenzene was co-deposited with celecoxib.³⁹ The resulting glasses exhibited high kinetic stability, similar to neat celecoxib, and this significantly impeded the photoisomerization of the azobenzene moiety. In a second example, *cis*- and *trans*-decalin³⁷ were co-deposited. PVD glass mixtures across the entire composition range showed high kinetic stability, comparable to that of neat *cis*-decalin. As a third example, with direct relevance for OLEDs, an iridium-containing emitter (8%) was co-deposited with a host material, 2,2',2''-(1,3,5-benzinetriyl)-tris(1-phenyl-1-*H*-benzimidazole). While the kinetic stability of the resulting glass was not directly evaluated, it can be inferred that highly stable mixed glasses were produced, based upon improvements in device lifetime for deposition at 0.85 T_g.⁴²⁻⁴³ This result indicates that simply knowing if a mixture can form a stable glass is an important design consideration. On the fundamental side, it is not obvious that a mixture should form a stable glass, even when the two components each individually form stable glasses. The surface equilibration mechanism explains stable glass formation based upon high surface mobility and equilibration that occurs during deposition.^{24, 44-47} But when two components are co-deposited, they may not have the same surface mobility at their common substrate temperature, particularly if their T_g values are significantly different. Other factors such as molecular shapes and the miscibility of the components will certainly influence the properties of the co-deposited glass.

To further our understanding of the properties of co-deposited PVD glasses, we conducted studies of *in situ* dielectric relaxation on vapor-deposited isomeric mixtures of *cis/trans*-decahydroisoquinoline (DHIQ). This is a relatively simple mixture of geometric isomers with

similar T_g values. In contrast to the previous work on decalin isomers, DHIQ has a significant dipole moment⁴⁸, and this is one factor that could influence the stability of co-deposited PVD glasses. An important feature of the DHIQ mixtures is the presence of prominent secondary relaxation processes that have been assigned to intramolecular ring-flip conformational changes.⁴⁸ Previous work on PVD glasses has shown that highly stable glasses generally have highly suppressed secondary relaxation processes³⁰⁻³², but up to this point, this property has not been investigated for molecules where the secondary relaxation is associated with internal conformational changes.

We investigated the kinetic stability and secondary relaxation suppression of three compositions of DHIQ: *trans*-DHIQ, 1:1 *cis/trans*-DHIQ, and 9:1 *cis/trans*-DHIQ. Each composition was deposited over a wide range of substrate temperatures (0.7 T_g - 1.0 T_g). We find that DHIQ forms highly stable glasses across the range of isomeric composition studied, and substrate temperature controls kinetic stability to a much greater extent than isomeric composition. In this respect, mixed glasses of DHIQ are similar to previously studied single component PVD glasses with transformation times exceeding the structural relaxation time τ_α by factors ranging from 10^3 to 10^5 . The (intramolecular) secondary relaxations of DHIQ are significantly suppressed in the most stable glasses, by factors ranging from 50 to 70%; this is comparable to the suppressions previously reported for other types of secondary relaxations.

Unexpectedly, the isothermal transformation of highly stable DHIQ glasses is quite different from previously studied stable glasses, in two respects. The isothermal transformation kinetics of highly stable DHIQ glasses cannot be interpreted in terms of a simple nucleation and growth model. That is, when fit to an Avrami model, the resulting exponents are generally greater than 4, suggesting that 3-dimensional growth at constant nucleation and growth rates is inadequate

1
2
3 to explain the observed behavior. In addition, depositing a highly stable glass on top of a liquid-
4 cooled glass did not have the expected effect of increasing the fraction of the transformation
5 process occurring via surface-initiated processes. We offer some highly speculative ideas for
6 interpreting these results.
7
8
9
10
11
12
13
14

15 Experimental

16
17 Mixed isomer DHIQ solutions were purchased from Sigma-Aldrich (96 % purity) and TCI
18 (98% purity). The structures of the individual isomers of DHIQ are shown in Figure 1. We
19 determined the composition of these mixtures using $^1\text{H-NMR}$, and they were found to be roughly
20 1:9 *cis/trans* for the material from Sigma-Aldrich and roughly 9:1 *cis/trans* for the material from
21 TCI. *Trans*-DHIQ (95% purity) was purchased from Atlantic Research Chemicals. Vapor-
22 deposited glasses were prepared in a home-built vacuum chamber with base pressure $<10^{-7}$ Pa. A
23 DHIQ sample with a particular isomeric composition was placed in a stainless-steel reservoir and
24 introduced into the chamber via a fine leak valve. 1:1 *cis/trans*-DHIQ glasses were deposited by
25 vaporizing a mixture with equal volumes of the 9:1 *cis/trans* and 1:9 *cis/trans* DHIQ materials. In
26 these experiments, we assumed that the two isomers have equal vapor pressures, and thus that the
27 PVD glass composition is equal to the reservoir composition. We checked this assumption by
28 comparing the composition in the reservoir before and after a series of depositions (which used a
29 significant fraction of the liquid); ^1H NMR spectrum revealed no change in reservoir composition.
30 The deposition rate (0.6 nm/s) was controlled to within 5% via the chamber pressure as indicated
31 by an ionization gauge.
32
33
34
35
36
37
38
39
40
41
42
43
44
45
46
47
48
49
50

51 Films were deposited onto interdigitated electrode devices, Abtech IME 1025.3-FD-Pt-U
52 and IME 1025.3-FD-Au-U, which are borosilicate glass substrates with two pairs of platinum or
53
54
55
56
57
58
59

gold microlithographically patterned (lift off) on the surface. For these devices, the electrodes are 10 microns in width and the gap between electrodes is also 10 microns. In our deposition chamber, one pair of electrodes is open to deposition and the other is covered such that no deposition occurs, to serve as a reference for our measurement. The electric field lines of the interdigitated electrode devices extend beyond the thickness of the film used in a typical experiment, which has the same effect as not fully filling a parallel plate capacitor. Therefore, the dielectric permittivities reported in this work are not absolute. DHIQ film thicknesses were determined by comparison with the saturation behavior of the dielectric signal of methyl-m-toluate (MMT) during deposition at fixed deposition rate, as described earlier⁴⁹. For each DHIQ deposition, the increase in the film thickness with time was monitored in two ways: by measuring the increase of the dielectric loss, and by measuring the increase in the heat capacity using a nanocalorimeter also present in the deposition chamber. The thickness and deposition rate for a given DHIQ deposition were calculated from these two measurements, making use of the MMT saturation measurement described above (and using the heat capacities and densities of DHIQ and MMT⁵⁰⁻⁵¹). Considering the uncertainties associated with these procedures, we expect the absolute film thicknesses and deposition rates reported here to be accurate to within 20%.

Two types of experiments were performed on glasses of DHIQ. For both types of experiments, the vacuum chamber was backfilled with 3×10^4 Pa of dry nitrogen after deposition to prevent desorption of the glasses during the subsequent temperature protocols. In the first type of experiment, a DHIQ glass prepared at a substrate temperature $\leq T_g$ was characterized during temperature cycling. The glass was heated at 5 K/min to transform the as-deposited glass into the supercooled liquid and then cooled at 5 K/min to prepare a liquid-cooled glass. This temperature cycle would be repeated 2-3 times to measure the response of the liquid-cooled glass and ensure

the as-deposited glass had fully transformed. During temperature cycling, the dielectric response of the glass was measured at 20 Hz. These experiments allow for quantification of the kinetic stability and secondary relaxation suppression of the vapor-deposited glasses. As illustrated below, the kinetic stability is assessed by the increased T_{onset} determined from the intersection of tangent lines drawn to the glassy response and the region where the loss rapidly increases upon transformation.

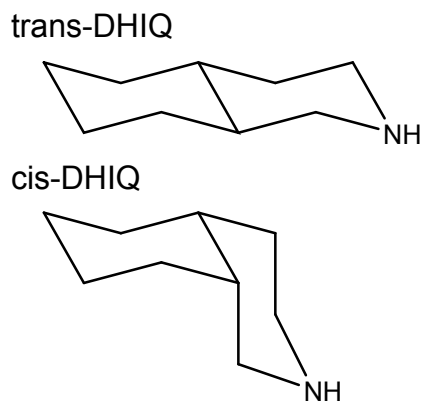


Figure 1. Structures of *trans*-DHIQ and *cis*-DHIQ ($\text{C}_9\text{H}_{17}\text{N}$), $T_g \approx 180$ K.

In the second type of experiment, a DHIQ glass would be deposited at the substrate temperature that provided the highest kinetic stability for each isomeric composition (near $0.86T_g$), and then characterized during isothermal annealing. The as-deposited glass was heated at 10 K/min to a temperature a few K above T_g at which point the temperature was held constant while measuring the dielectric response at a single frequency. A variation of this isothermal transformation experiment involved depositing a second film on top of a liquid-cooled glass. These isothermal experiments provide information on the kinetic stability of vapor-deposited glasses and information about the mechanism by which these glasses transform into the supercooled liquid.

Results

Single-Frequency Temperature-Cycling Experiments

Single-frequency temperature-cycling experiments were performed to survey the effect of composition and deposition temperature on the kinetic stability of vapor-deposited glasses of DHIQ mixtures. Figure 2 shows representative temperature-cycling experiments for stable glasses of each of the three isomeric compositions. The primary features of these experiments are the increased onset temperature for the transformation into the supercooled liquid, and the reduced loss amplitude for the as-deposited glass (first scan) relative to the liquid-cooled glass (second and third scans). The large increase in the onset temperature for all three compositions is an indication that all compositions form glasses with high kinetic stability. Past work on other types of secondary relaxations has shown that suppressed secondary relaxations are generally associated with vapor-deposited glasses.^{30-32, 52} A subtler feature of these experiments is the change of shape of the secondary relaxations with isomeric composition. As the fraction of *cis*-DHIQ is decreased, secondary relaxations become less separated from the primary relaxation and increase in amplitude relative to the primary relaxation which can be seen in the progression from Figure 2a – 2c. We did not observe crystallization during temperature cycling with the exception of *trans*-DHIQ glasses deposited at or above T_g which crystallized prior to the end of the three-scan sequence shown in Figure 2. Results from experiments showing crystallization are not reported.

At low deposition temperatures, the vapor-deposited glasses of DHIQ become less kinetically stable, while maintaining a moderate amount of secondary relaxation suppression. Representative examples of these 9:1 *cis/trans*-DHIQ and 1:1 *cis/trans*-DHIQ glasses are shown in Figure 3. These two compositions form kinetically unstable glasses at low deposition

1
2
3 temperatures, as indicated by the onset temperature being less for the as-deposited glass than for
4 the liquid-cooled glass. *Trans*-DHIQ was not included in this figure because at similar substrate
5 temperatures relative to T_g , *trans*-DHIQ continued to show enhanced kinetic stability.
6
7
8
9

10 The results from all single-frequency temperature-cycling experiments like Figures 2 and
11 3 are compiled in Figure 4. Figure 4a indicates that the substrate temperature has a stronger
12 influence on the kinetic stability than isomeric composition, particularly for T_{sub}/T_g at or above
13 0.85. The optimum substrate temperature to produce the most stable glasses is between 0.85 and
14 0.90 T_g which is consistent with previous work on single component PVD glasses.^{14, 53-55} As the
15 deposition temperature is lowered, the glasses containing *cis*-DHIQ become kinetically unstable,
16 i.e., the T_{onset} of the vapor-deposited glass is below that of the liquid-cooled glass. In contrast, the
17 *trans*-DHIQ glasses retain at least some enhanced kinetic stability and also maintain a high degree
18 of secondary relaxation suppression.
19
20
21
22
23
24
25
26
27
28
29

30 Figure 4b indicates significant suppression of secondary relaxations for all DHIQ glasses,
31 for depositions that produce the most stable glasses. This connection and the absolute magnitude
32 of the secondary relaxation suppression is consistent with previous work on single component
33 PVD glasses.³⁰⁻³¹ A strong correlation between high kinetic stability and suppression of secondary
34 relaxations has been observed directly in at least one system³¹⁻³² and is likely the result of
35 secondary relaxations serving as an indicator of the amount of residual motion in the glass.
36
37
38
39
40
41
42
43
44

45 The trends shown in Figure 4 are broadly consistent with the surface equilibration
46 mechanism⁴⁴. As a further check on the role of surface equilibration in these experiments, we
47 performed one experiment (on 1:1 *cis/trans*-DHIQ) in which the deposition rate was lowered by
48 one order of magnitude. As expected from the surface equilibration mechanism, the kinetic
49 stability and secondary relaxation suppression both increased relative to that observed for a glass
50
51
52
53
54
55
56
57
58
59
60

1
2
3 deposited at the same substrate temperature at the normal rate. These results are shown in Figure
4
5 S1 in the Supplemental Material.
6

7
8 In Figure 3, the observation that the dielectric loss of the as-deposited glass (red lines)
9 crosses the response of the liquid-cooled glass (blue/gray lines) was unexpected. We explored this
10 behavior in a separate experiment on an unstable glass. During the first heating cycle of the as-
11 deposited glass, temperature ramping was stopped after the as-deposited loss value crossed above
12 the liquid-cooled value. During the subsequent isothermal hold, we observed that the high loss
13 state decayed over the course of a few minutes to the value of the liquid-cooled glass. After a
14 further two hours at constant temperature, further temperature cycling gave results consistent with
15 an ordinary glass aged for 2 hours indicating the glass completely transformed below T_g . (See
16 Figure S2 in Supporting Information.)
17
18
19
20
21
22
23
24
25
26
27
28
29
30
31
32
33
34
35
36
37
38
39
40
41
42
43
44
45
46
47
48
49
50
51
52
53
54
55
56
57
58
59
60

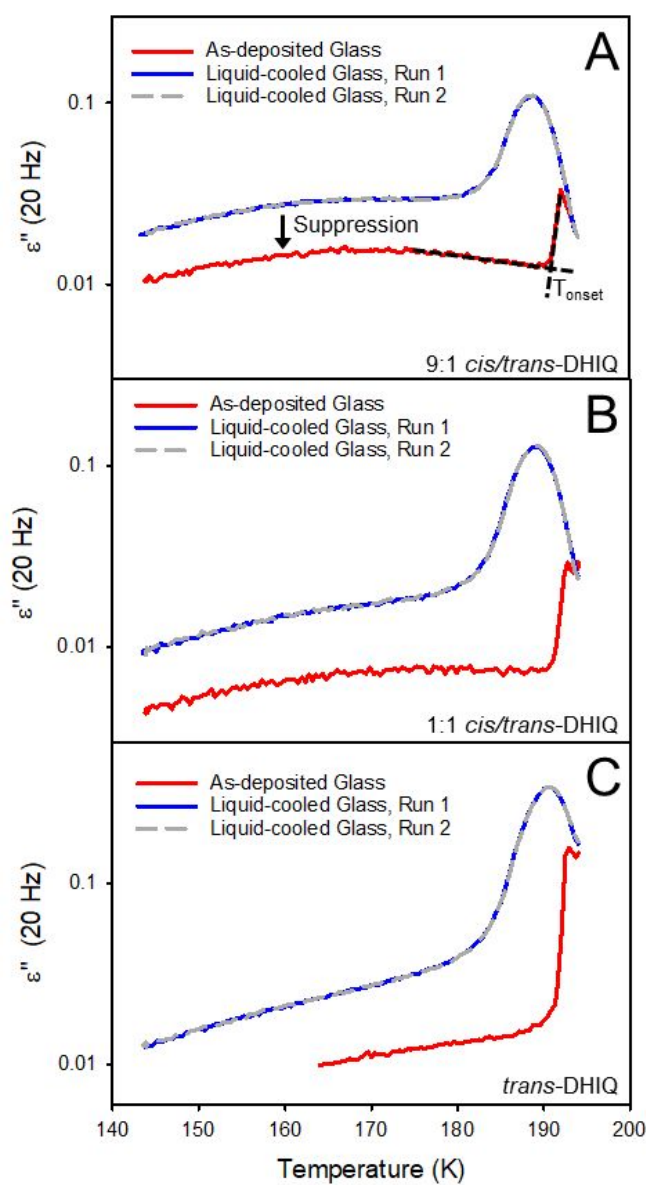


Figure 2. Dielectric loss at 20 Hz as a function of temperature for kinetically stable vapor-deposited DHIQ mixtures. A) 9:1 *cis/trans*-DHIQ ($T_{dep} = 160$ K), B) 1:1 *cis/trans* DHIQ ($T_{dep} = 160$ K), C) 100% *trans*-DHIQ ($T_{dep} = 158$ K). In all three cases the as-deposited glasses display enhanced kinetic stability and secondary relaxation suppression relative to the liquid-cooled glass (runs 1 and 2). Heating and cooling rates were 5 K/min. Film thickness ≈ 700 nm.

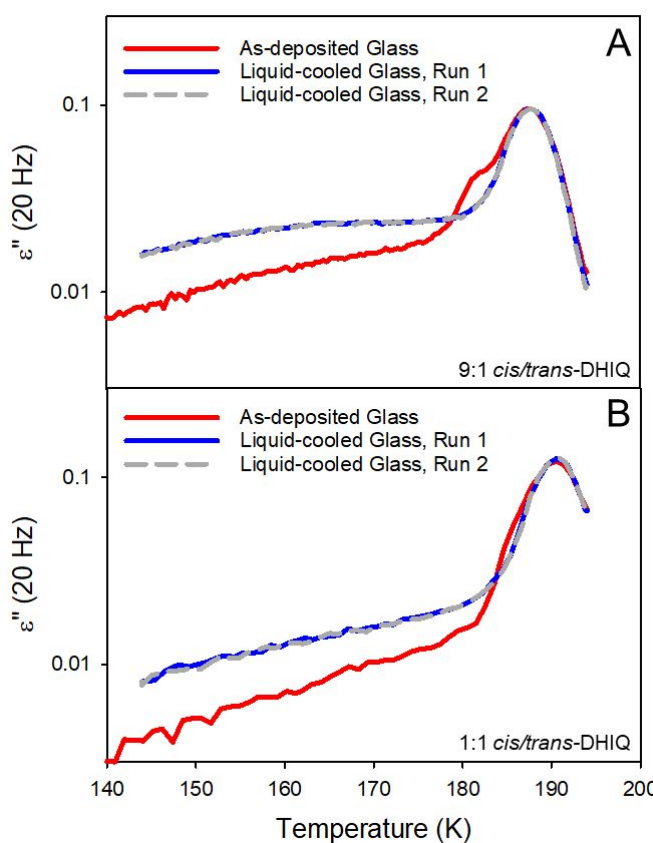


Figure 3. Dielectric loss at 20 Hz as a function of temperature for kinetically unstable vapor-deposited DHIQ mixtures prepared at temperatures near $0.75T_g$. A) 9:1 *cis/trans*-DHIQ ($T_{\text{dep}} = 130 \text{ K}$, B) 1:1 *cis/trans* DHIQ ($T_{\text{dep}} = 131 \text{ K}$). In both cases, the as-deposited glass displays a sharp increase in loss amplitude at a lower temperature than the liquid-cooled glass (runs 1 and 2). Heating and cooling rates were 5 K/min. Film thickness $\approx 700 \text{ nm}$.

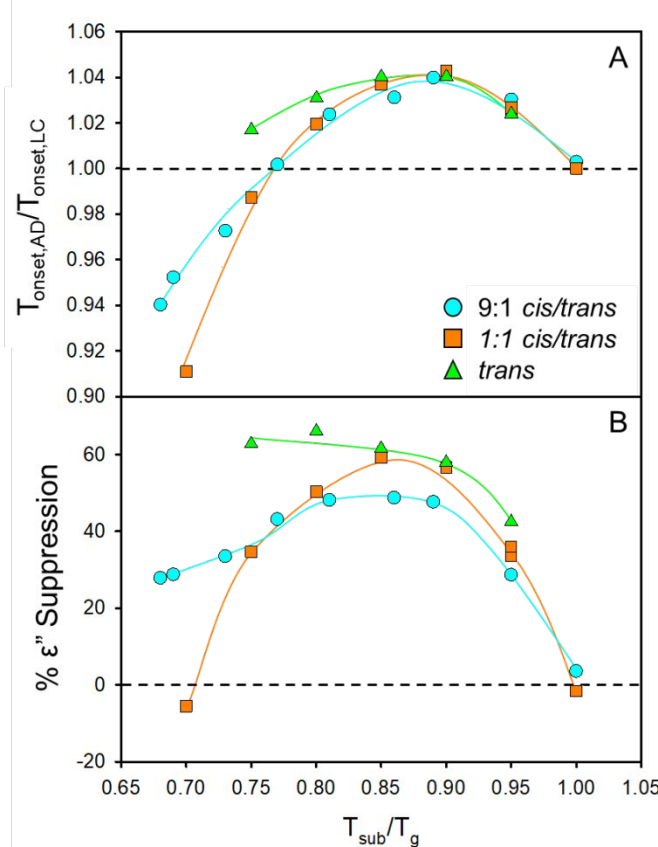


Figure 4. Kinetic stability (A) and suppression of secondary relaxations (B) for vapor-deposited DHIQ glasses as a function of substrate temperature scaled by T_g . $T_{\text{onset,AD}}/T_{\text{onset,LC}}$ is the ratio of the onset temperatures obtained using the tangent method for the as-deposited and liquid-cooled glasses respectively. The y-axis was calculated from the ratio of the 20 Hz loss amplitude of the as-deposited glass to the liquid-cooled glass at $T_g - 10$ K. Lines are a guide to the eye.

Isothermal Annealing Experiments

Single-layer Films: The results of representative isothermal transformation experiments are shown in Figure 5. In these experiments, the as-deposited glass is brought to the annealing temperature at 10 K/min and then held isothermally until the transformation into the supercooled liquid is complete; the definition of the isothermal transformation time is shown in Figure 5a. Figure 5 shows that glasses for all three isomeric mixtures are highly stable, as the transformation times scaled by τ_α of the resulting supercooled liquid are $\approx 10^4$. Each of the transformation curves was fitted to the Avrami model, $Y = 1 - \exp(- (Kt)^m)$, where Y is the fraction of the film that

1
2
3 has transformed into the supercooled liquid, t is the time since reaching the annealing temperature,
4 and K and m are fitting parameters. As we discuss below, for most of the experiments shown in
5 Figures 5 – 7, fitting the transformation curves to this model provides reasonable fits only when
6 the exponent m is allowed to assume values > 4 ; this differs from previous work on TPD⁵⁶ and
7 IMC⁵⁷.
8
9

10 The 9:1 *cis/trans*-DHIQ mixture, shown in Figure 5a, shows transformation behavior that
11 is mostly consistent with features observed in single component stable glass forming systems.
12 Immediately after reaching the annealing temperature, the loss amplitude increases linearly for a
13 few hundred seconds (tens of thousands of τ_a). Previous work has shown that a linear
14 transformation behavior occurs when the transformation proceeds at a constant rate from the
15 initiating surface.^{44, 58-63} In a second stage in Figure 5a, the loss amplitude increases at a much
16 faster rate until the film is completely transformed into the supercooled liquid at which point the
17 dielectric response becomes constant.⁶⁴ Previous work has shown that this behavior is associated
18 with the bulk transformation of the glass. For the 9:1 *cis/trans*-DHIQ glass, the initial linear
19 transformation region was omitted from the fitting because the Avrami equation is used to model
20 the bulk transformation. In Figure 5a, we see that the Avrami fit to the second stage of the
21 transformation produces an m value of 6.46. The value of m carries special significance because,
22 in the context of the Avrami model, phase transitions in three dimensional systems lead to $m \leq 4$.
23
24 Further comments on this point will be made in the discussion section.
25
26

27 The isothermal transformation of the 1:1 *cis/trans*-DHIQ mixture, shown in Figure 5b,
28 shows behavior which appears qualitatively different than Figure 5a, as it appears to lack a linearly
29 increasing region immediately after reaching the annealing temperature. The transformation time
30 is significantly shorter in Figure 5b, so it is possible that surface-initiated transformation is not
31
32
33
34
35
36
37
38
39
40
41
42
43
44
45
46
47
48
49
50
51
52
53
54
55
56
57
58
59
60

1
2
3 easily observed before the bulk transformation begins. For the 1:1 *cis/trans*-DHIQ mixture, the
4
5 Avrami fit describes the data reasonably well with an exponent of 4.8; fixing the exponent to 4
6
7 does not significantly alter the quality of the fit.
8
9

10 For the isothermal transformation of *trans*-DHIQ, shown in Figure 5c, we again observe
11
12 an initial linear transformation region. A high value of the Avrami exponent was found for this
13
14 transformation ($m = 9.18$). If the initial linear region is excluded from the fit, an even larger value
15
16 of m is obtained. For this experiment, fixing the exponent to 4 does not reproduce the sharp nature
17
18 of the observed transition (see Figure S5 in Supporting Information).
19
20

21 For reference, if the experiment shown in Figure 5 is performed on a liquid-cooled glass, a
22
23 constant signal is obtained, because the glass fully transforms into the supercooled liquid before
24
25 the annealing temperature is reached.
26
27
28
29
30
31
32
33
34
35
36
37
38
39
40
41
42
43
44
45
46
47
48
49
50
51
52
53
54
55
56
57
58
59
60

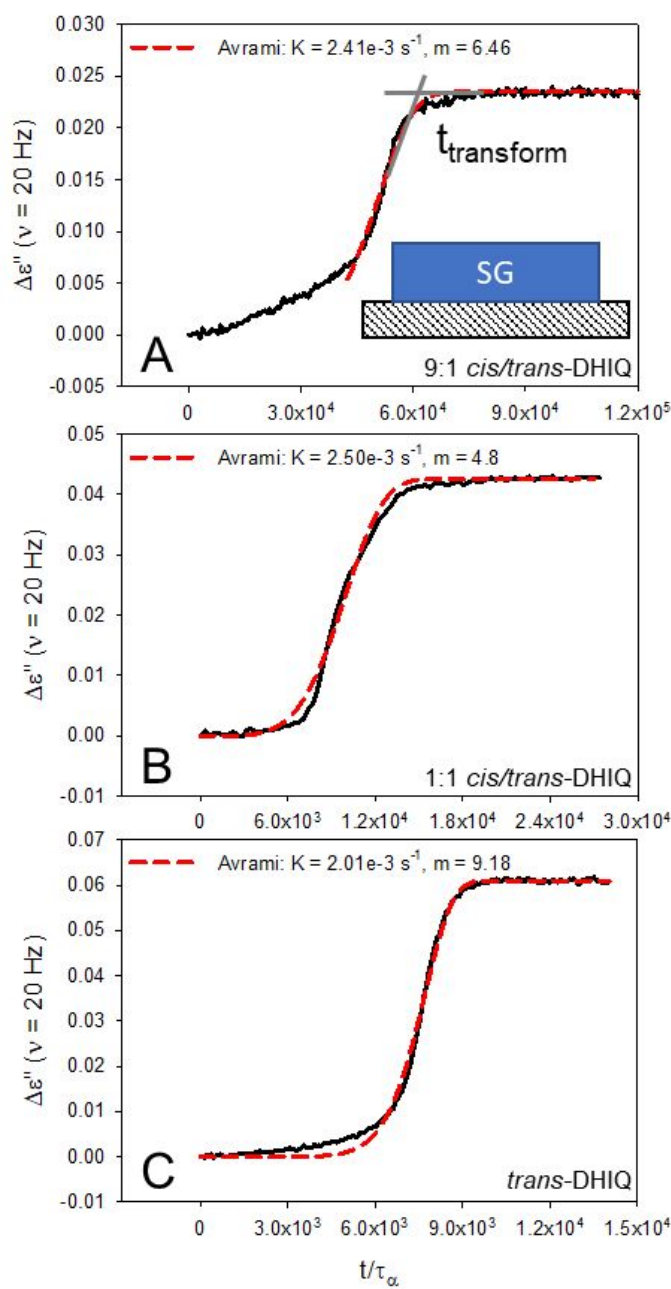


Figure 5. Isothermal annealing experiments for single layer vapor-deposited glasses of isomeric mixtures of DHIQ. A) 9:1 *cis/trans*, B) 1:1 *cis/trans*, C) pure *trans*-DHIQ. The vertical axis is the change in the dielectric signal at 20 Hz since reaching the annealing temperature. The horizontal axis is the time since reaching the annealing temperature scaled by the τ_a of the supercooled liquid (measured after the transformation had completed). Transformation curves were fit to an unconstrained Avrami model with the resulting parameters listed in the respective panels. The amount of the curve that the fit covers represents the range of data used in the fit. Films were all approximately 750 nm thick. Panel A inset: schematic of layer geometry with a stable glass (SG)

1
2
3 on top of the interdigitated electrode device. $T_{\text{anneal}} = 185$ K, 184 K, and 184 K for each panel
4 respectively. $T_{\text{dep}} = 160$ K, 160 K, and 158 K for each panel respectively.
5
6
7

8 **Two-layer glasses:** The films represented in Figure 5 were utilized in a second set of
9 experiments performed on the same day. After those glasses had transformed into the supercooled
10 liquid, they were cooled back down to the temperature at which they had been deposited to produce
11 an ordinary glass. A new stable glass was deposited on top of the ordinary glass. The same
12 isothermal annealing procedure was used on these layered glasses, and the results are shown in
13 Figure 6. The transformation of the underlying ordinary glasses is not visible in Figure 6 because
14 they fully transform before the annealing temperature is reached, and their contribution to the
15 signal is therefore subtracted away. This type of two-layer glass has been used in previous work
16 to initiate a growth front at the buried interface in addition to the front that begins at the vacuum
17 interface.⁶⁵ Based upon previous work, we expect a two-layer glass to show a more prominent
18 initial linear transformation (because now two surface-initiated fronts are growing), but we expect
19 the final bulk transformation not to be influenced. However, for DHIQ, these two-layer glass
20 experiments showed several unexpected results.
21
22
23
24
25
26
27
28
29
30
31
32
33
34
35
36

37 In Figure 6a, we show the isothermal transformation of a two-layer glass of 9:1 *cis/trans*-
38 DHIQ. Surprisingly, the initial linear increase of the loss amplitude observed in Figure 5a is absent
39 when an ordinary glass of this material is used as the substrate. The overall transformation time is
40 very nearly the same here and in Figure 5a. The Avrami exponent obtained for the two-layered
41 film ($m = 9.75$) is larger than that obtained for the single-layer film, and this is not a consequence
42 of the different fitting ranges; using a similar data range as that of Figure 5a still produces a value
43 of m greater than 9.
44
45
46
47
48
49
50
51
52

The 1:1 *cis/trans*-DHIQ layered glass (Figure 6b) shows a very slow initial transformation (comparable to that shown in Figure 5b) followed by a more rapid completion of the transformation. However, the overall transformation time is longer in Figure 6b, contrary to our expectation. The unusual shape of this transformation is not well fit by the Avrami model. In contrast to the two isomeric mixtures, the *trans*-DHIQ layered film (Figure 6c) shows no appreciable difference compared to the single layer stable glass.

A control experiment was performed in light of the unusual Avrami exponents obtained in these experiments. We performed a few isothermal transformations while monitoring the dielectric loss at two different frequencies, and this data is included in the Supporting Information as Figures S3 and S4. No significant differences in the transformation kinetics were observed. With a measurement at a single frequency, it might be imagined that the dielectric signal was being significantly influenced by secondary relaxations. Since two well-separated frequencies agree in their characterization of the phase transformation kinetics, we find this possibility unlikely. In contrast, this control experiment supports the view that the increased dielectric signals in Figures 5 and 6 accurately reflect the growth of the supercooled liquid fraction with time.

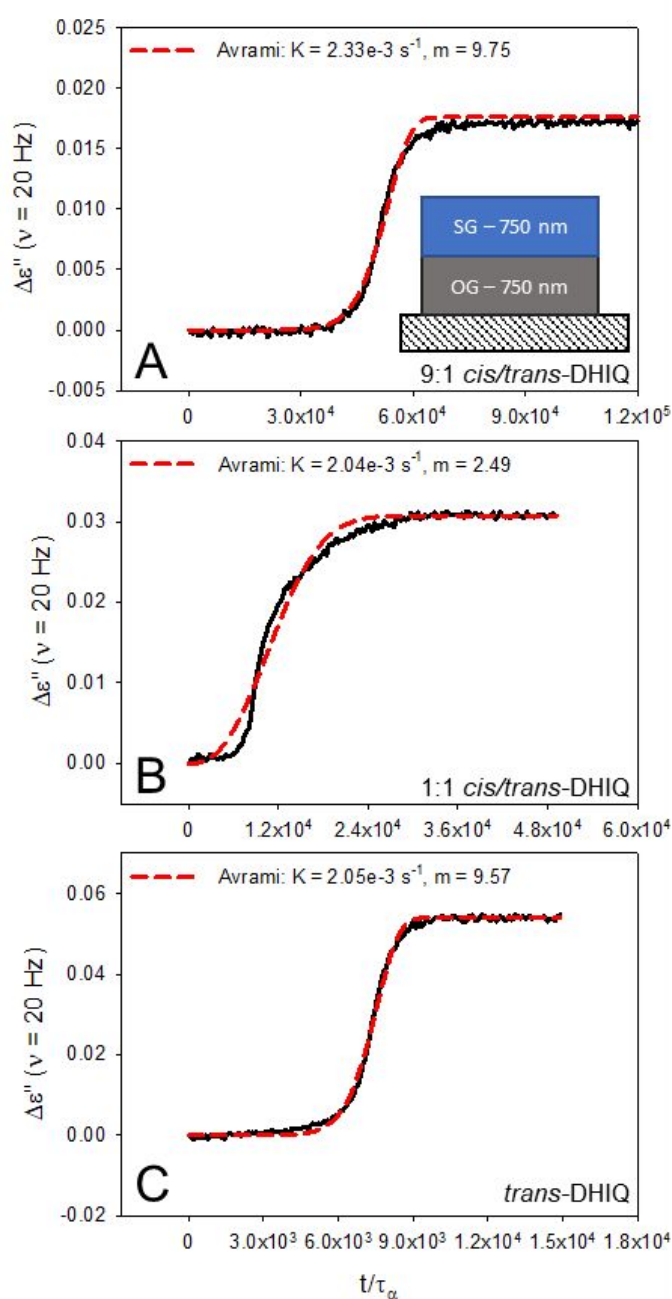


Figure 6. Isothermal annealing experiments for vapor-deposited glasses of isomeric mixtures of DHIQ deposited on top of an ordinary glass of the same material. A) 9:1 *cis/trans*, B) 1:1 *cis/trans*, C) pure *trans*-DHIQ. Stable films were all approximately 750 nm thick bringing the total film thickness to 1.5 μ m. The meaning of the axes is the same as in Figure 5. Top panel inset: schematic of layer geometry with a stable glass (SG) on top of an ordinary glass (OG). $T_{\text{anneal}} = 185$ K, 184 K, and 184 K for each panel respectively. $T_{\text{dep}} = 160$ K, 160 K, and 158 K for each panel respectively.

Transition from surface-initiated growth front to bulk transformation:

Further isothermal transformation experiments were performed on the 1:1 *cis/trans*-DHIQ to clearly separate the surface-initiated and bulk transformation mechanisms. Here glasses of different thicknesses were deposited directly on the substrate to identify the fraction of the film that transforms via the growth front mechanism. The transformation data is shown in Figure 7. We observe a common, linear evolution of the dielectric signal with time immediately after reaching the annealing temperature that is consistent with growth front behavior. We also observe that all films complete their transformation at approximately the same time, consistent with a transition to a bulk transformation mechanism. From the rate of change in dielectric signal and the film thicknesses, we can determine the growth front velocity to be 0.22 ± 0.04 nm/s for this particular deposition and annealing temperature. The crossover length (characterizing the transition from surface-initiated to bulk transformation) can also be observed to be 90 ± 20 nm based on the thickness of the films and the fraction of the film that transforms before the linear transformations diverge from each other.

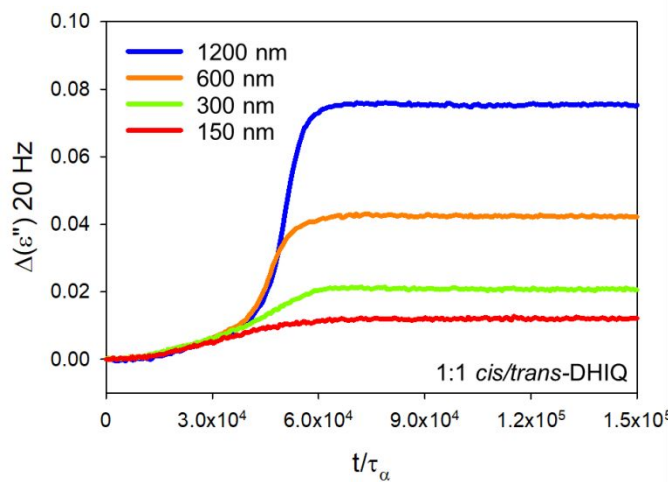


Figure 7. Isothermal annealing experiments for vapor-deposited glasses of 1:1 *cis/trans*-DHIQ of various thicknesses, $T_{\text{anneal}} = 186 \text{ K}$ $T_{\text{dep}} = 155 \text{ K}$. The meaning of the axes is the same as Figures 5 and 6.

Discussion

1
2
3 By some measures, PVD glasses of isomeric mixtures of DHIQ are similar to dozens of
4 other stable glass-forming systems, but by other measures, the results reported here are unique.
5
6 We will begin by discussing the features of DHIQ that are most consistent with previous work on
7
8 PVD glasses, and then we will explore those features which require novel explanations.
9
10
11
12
13
14

15 **Glass stability as a function of composition and substrate temperature**

16

17 The number of systems that form stable glasses when prepared by PVD has been steadily
18 increasing since the initial discovery of stable glasses. The surface equilibration mechanism that
19 controls their formation is well established and arises from the greater mobility which molecules
20 at the surface of the growing film have relative to the molecules in the bulk. The features of Figure
21 4a are qualitatively similar to previously reported results for single component systems⁵³. The
22 stability of the glasses increases as the deposition temperature is lowered to $0.9T_g$. The overlap of
23 all three compositions near T_g indicates that composition plays little role in the ability to form
24 stable glasses of the neat DHIQ and its mixtures. This result provides additional evidence that
25 systems with miscibility, similar sizes, and similar T_g values are not prevented from forming stable
26 glasses. In this respect the results presented here for DHIQ are similar to previously-published
27 work on mixtures of decalin (a structural analog to DHIQ).³⁷ As the isomers of DHIQ have much
28 larger dipole moments than the decalin isomers, it is also clear the this factor does not preclude the
29 formation of highly stable glass mixtures.
30
31
32
33
34
35
36
37
38
39
40
41
42
43
44
45
46
47
48
49
50
51
52
53
54
55
56
57
58
59
60

At lower temperatures, Figure 4a shows that the composition impacts kinetic stability. The mixed DHIQ glasses become unstable at the lowest substrate temperatures studied, where *trans*-DHIQ retains some stability. In contrast, decalin mixtures did not show a significant difference between the kinetic stability vs deposition temperature behavior for *cis*-decalin and 1:1 *cis/trans*-

1
2
3 decalin.³⁷ However, not all single component systems have the same stable glass formation
4 range,⁶⁶ so the origin of the differences in Figure 4a is not clear. One could interpret the data in
5 Figure 4a to indicate that surface mobility is higher for *trans*-DHIQ than for the mixed systems in
6 this temperature range, but we have no independent test of this.
7
8

9 In Figure 4b, we show the suppression of secondary relaxations observed in these DHIQ
10 glasses. Secondary relaxations are the small amplitude molecular motions that persist in the glassy
11 state. The secondary relaxations of DHIQ have been identified as originating from *intramolecular*
12 conformation changes⁴⁸. This is the first time that a stable glass has been prepared from such a
13 molecule, and it is interesting that such a secondary relaxation process is significantly hindered by
14 stable glass formation, with the amplitude of the process being suppressed by up to 70%.
15 Suppression of this magnitude is consistent with higher packing density, and similar levels of
16 suppression have been reported for other molecules, including those in which the secondary
17 relaxation process is entirely *intermolecular* in origin^{30-32, 52}. In Figures 2 and 3, the appearance of
18 the secondary relaxation is shown to depend on isomeric composition with a greater fraction of
19 *cis*-DHIQ resulting in a stronger, more separated peak. In previous work on DHIQ, the isomeric
20 composition was either unknown or not reported.⁶⁷⁻⁶⁸ Ideally, one would deconvolute the dielectric
21 spectra of DHIQ mixtures to observe the effect glass stability had on the secondary relaxations of
22 each component. However, developing a procedure to do that unambiguously is a challenge that
23 is outside the scope of this work.
24
25

26 The surface-initiated transformation mechanism transforms stable glasses as a constant
27 velocity front that converts stable glass into supercooled liquid. Sufficiently thin films can
28 completely transform by this mechanism, while for thick films the surface-initiated process will
29 be disrupted by the bulk transformation after the front has propagated a distance known as the
30
31
32
33
34
35
36
37
38
39
40
41
42
43
44
45
46
47
48
49
50
51
52
53
54
55
56
57
58
59
60

1
2
3 crossover length. The crossover length for PVD glasses of 1:1 *cis/trans*-DHIQ is 90 ± 20 nm (Figure
4
5), which is about an order of magnitude smaller than the values observed for several other stable
6 glasses. For comparison, highly stable PVD glasses of tris-naphthylbenzene and indomethacin
7 have been reported to have crossover lengths about an order of magnitude larger (~ 1000 nm).⁶⁹⁻⁷¹
8
9 Recent work by Rodriguez-Tinoco et al. has argued for a strong connection between the surface
10 and bulk transformation processes of stable glasses.⁶⁹ Using their analysis, we calculate that
11 the interfacial width of the transformation front for DHIQ is about 1 nm, which is in the 1-4 nm
12 range observed for other highly stable glasses. Thus, the relationship between surface and bulk
13 transformation that we observe here for DHIQ is not so different from those of other PVD glasses.
14
15

16 In the cases of indomethacin,⁵⁷ the crossover length has been interpreted as the
17 approximate distance between nucleation sites of the supercooled liquid within the bulk of the
18 film. This interpretation has been challenged by recent simulations, showing that the inferred
19 distances may be too large, by perhaps a factor of two.⁷²
20
21

35 Comparison of single-layer and double-layer glass films.

36
37 The most surprising results from the isothermal annealing experiments on highly stable
38 DHIQ glasses are the change in growth front behavior from the single-layer films to the two-layer
39 films, and the results of fitting these data to an Avrami model. Figure 5a shows an apparent growth
40 front that initiates shortly upon reaching the annealing temperature which then transitions to a bulk
41 transformation mechanism. Unexpectedly, when a second stable film is deposited onto an ordinary
42 film the growth front apparently disappears and only the bulk transformation remains (Figure 6a).
43 This is exactly the opposite of the expected behavior. In previously published work on other
44 systems, the addition of an ordinary glass underlayer has been used to ensure that a growth front
45
46
47
48
49
50
51
52
53
54
55
56
57
58
59

1
2
3 initiates from the bottom of the film (at the interface between the stable and ordinary glass) and
4 propagates toward the center of the film.^{65, 73} Thus, we expected that two-layer glasses should
5 transform more quickly (or at the same rate) as single-layer glasses. We do not have a satisfying
6 explanation for these observations but provide some tentative ideas below.
7
8

9 Conceivably, this unusual behavior might be explained with the idea that the growth fronts
10 observed in Figures 5 and 7 were initiated at the IDE substrate, and that no growth front occurred
11 from the opposing free surface. This would be surprising as free surfaces have been observed to
12 initiate transformation fronts for other stable glass systems, and this has been explained as the
13 natural consequence of the high mobility at the free surface. One of the control experiments
14 described above can be viewed as a test for high surface mobility. As shown in Figure S1, we
15 vapor-deposited a glass of 1:1 cis/trans-DHIQ at 1/10 the deposition rate used for other samples
16 reported here and found that the more slowly deposited glass exhibited greater kinetic stability and
17 secondary relaxation suppression presumably due to the increased equilibration time afforded to
18 molecules at the free surface. This result is consistent with the surface equilibration mechanism
19 and indirectly indicates a highly mobile surface. We expect that a highly mobile surface can initiate
20 transformation of a stable glass, so this control experiment argues against the tentative explanation
21 advanced in this paragraph.
22
23

24 The Avrami model has been used in the past to describe the bulk transformation of vapor-
25 deposited glasses.^{56-57, 74} In these cases, the fitted values of m were less than 4, which is the
26 maximum value expected for a phase transformation in three dimensions. In contrast, we can see
27 in Figures 5-7 that the transformations of DHIQ glasses generally are fit with exponents greater
28 than 4, and these values defy simple interpretation. Vila-Costa *et al.* performed detailed
29 experiments on the bulk transformation of TPD and interpreted their results using the Avrami
30
31
32
33
34
35
36
37
38
39
40
41
42
43
44
45
46
47
48
49
50
51
52
53
54
55
56
57
58
59
60

1
2
3 model.⁵⁶ They studied thin films and films thicker than the crossover length. For the thin films,
4 they observed an Avrami exponent of 2 which they attribute to preformed nuclei growing in two
5 dimensions because the spacing between nuclei is much larger than the film's thickness. Films
6 thicker than the crossover length show an exponent near 3 which is interpreted as 3D growth of
7 preformed nuclei. One difference between that study and the current work is that the TPD films
8 were capped from above and below with a higher T_g material to prevent the initiation of growth
9 fronts, but we do not have a hypothesis for why this difference would be consequential.
10
11

12 The Avrami model includes these relevant assumptions: nucleation occurs at a constant
13 rate, the growth rate is isotropic, and the growth rate is independent of the extent of the
14 transformation. We now briefly speculate as to how these assumptions might not be valid for PVD
15 glasses of DHIQ. If the nucleation rate increased with time, a fit to the standard Avrami model
16 could yield m values larger than 4. As PVD glasses are generally anisotropic,³³ it is possible that
17 the growth rates are not isotropic, although no experimental data is available on this point; we have
18 not characterized the anisotropy of PVD glasses of DHIQ. Similarly, if the growth rate increased
19 with time, larger m values could result. A very recent simulation work addresses one of these
20 possibilities, reporting that the growth front velocity is not constant in time during the isothermal
21 transformation of a stable glass, but rather accelerates in a manner that gives rise to an Avrami
22 exponent of greater than 4.⁷² The simulations report that bubbles of supercooled liquid initially
23 grow slowly because they are under pressure. These simulation results could offer a possible
24 explanation for the large Avrami exponents reported here, but further work would be needed to
25 understand why the result has only been observed for DHIQ and not other stable glass systems.
26
27

28 As a potentially important point related to the large Avrami exponents observed here, we
29 note that this work is the only work to our knowledge that calculates Avrami parameters from
30
31
32
33
34
35
36
37
38
39
40
41
42
43
44
45
46
47
48
49
50
51
52
53
54
55
56
57
58
59
60

1
2
3 dielectric relaxation data. Previous work on Avrami parameters of transforming vapor-deposited
4 glasses was done using calorimetric techniques.^{56-57, 69} These different techniques are sensitive to
5 different aspects of the system. For example, for dielectric relaxation, one could be concerned that
6 the y axis in Figures 5-7 is not simply reporting the fraction of supercooled liquid in the sample
7 but might be also reporting on changes in the secondary relaxation. For our measurements, we do
8 not expect that this is the case. As described above, we performed a few transformation
9 experiments while monitoring at two different frequencies (Figures S3 and S4). No significant
10 differences in the transformation kinetics were observed, consistent with the view that our
11 observation is only sensitive to the growth of the α relaxation process and thus characterizes the
12 fraction of the supercooled liquid.
13
14
15
16
17
18
19
20
21
22
23
24
25
26
27
28
29
30

31 Conclusion

32

33 In this work, we use *in situ* dielectric relaxation to characterize the stable glass forming
34 ability of vapor-deposited mixtures of *cis*- and *trans*-DHIQ. At the optimum deposition conditions,
35 the kinetic stabilities of pure and mixed glasses were quite high and comparable to many single-
36 component stable glass formers. Isothermal transformation times of the most stable glasses of each
37 composition were found to be $>\approx 10^4 \tau_\alpha$. Secondary relaxations, which arise from intramolecular
38 conformation changes, were substantially suppressed in films of all compositions. In addition, the
39 shape of the secondary relaxation process was shown to depend on composition.
40
41

42 In addition, PVD glasses of DHIQ showed unusual results for the transformation behavior
43 for layered films comprised of stable and ordinary layers. The growth front behavior of the stable
44 glasses is unaffected or diminished by the presence of an ordinary glass underlayer. This is in
45
46
47
48
49
50
51
52
53
54
55
56
57
58
59
60

1
2
3 contrast to previous studies where ordinary glass layers initiate growth fronts with no induction
4 time. In addition, the time dependence of the transformation is not consistent with a simple
5 nucleation and growth interpretation. Further work will be required to understand this unusual
6 transformation behavior.
7
8
9
10
11
12
13
14

15 Supporting Information

16

17 Supporting information contains results regarding experiments exploring kinetic stability of
18 glasses deposited at lower deposition rates, transformation of kinetically unstable glasses, our
19 Avrami analysis at multiple frequencies, and the inability of the standard Avrami model to
20 reproduce the shape of our glass transitions.
21
22
23
24
25
26
27

28 Acknowledgements

29

30 We thank the U.S. National Science Foundation (CHE 1854930 and CHE 2153944) for support of
31 this work. We are grateful to Heike Hofstetter for assistance with NMR characterization of DHIQ
32 mixtures.
33
34
35
36

37 References

38

39
40
41
42 1. Debenedetti, P. G.; Stillinger, F. H., Supercooled liquids and the glass transition. *Nature*
43 **2001**, *410* (6825), 259-67.
44
45 2. Lubchenko, V.; Wolynes, P. G., Theory of structural glasses and supercooled liquids.
46 *Annual review of physical chemistry* **2007**, *58*, 235-66.
47
48 3. Ediger, M. D.; Harrowell, P., Perspective: Supercooled liquids and glasses. *The Journal of*
49 *chemical physics* **2012**, *137* (8), 080901.
50
51 4. Royall, C. P.; Williams, S. R., The role of local structure in dynamical arrest. *Physics*
52 *Reports* **2015**, *560*, 1-75.
53
54 5. Tanaka, H., General view of a liquid-liquid phase transition. *Physical Review E* **2000**, *62*
55 (5), 6968-6976.
56
57 6. Coslovich, D.; Pastore, G., Understanding fragility in supercooled Lennard-Jones
58 mixtures. I. Locally preferred structures. *The Journal of chemical physics* **2007**, *127* (12), 124504.
59
60

1
2
3
4
5
6
7
8
9
10
11
12
13
14
15
16
17
18
19
20
21
22
23
24
25
26
27
28
29
30
31
32
33
34
35
36
37
38
39
40
41
42
43
44
45
46
47
48
49
50
51
52
53
54
55
56
57
58
59
60

7. Palmer, J. C.; Martelli, F.; Liu, Y.; Car, R.; Panagiotopoulos, A. Z.; Debenedetti, P. G., Metastable liquid-liquid transition in a molecular model of water. *Nature* **2014**, *510* (7505), 385-8.
8. Zhu, M.; Yu, L., Polyamorphism of D-mannitol. *The Journal of chemical physics* **2017**, *146* (24), 244503.
9. Kobayashi, M.; Tanaka, H., The reversibility and first-order nature of liquid-liquid transition in a molecular liquid. *Nature communications* **2016**, *7*, 13438.
10. Berthier, L.; Charbonneau, P.; Coslovich, D.; Ninarello, A.; Ozawa, M.; Yaida, S., Configurational entropy measurements in extremely supercooled liquids that break the glass ceiling. *Proceedings of the National Academy of Sciences of the United States of America* **2017**, *114* (43), 11356-11361.
11. Liu, T.; Cheng, K.; Salami-Ranjbaran, E.; Gao, F.; Glor, E. C.; Li, M.; Walsh, P. J.; Fakhraai, Z., Synthesis and high-throughput characterization of structural analogues of molecular glassformers: 1,3,5-trisarylbenzenes. *Soft matter* **2015**, *11* (38), 7558-66.
12. Bhattacharya, D.; Sadtchenko, V., Enthalpy and high temperature relaxation kinetics of stable vapor-deposited glasses of toluene. *The Journal of chemical physics* **2014**, *141* (9), 094502.
13. Smith, R. S.; May, R. A.; Kay, B. D., Probing Toluene and Ethylbenzene Stable Glass Formation Using Inert Gas Permeation. *The journal of physical chemistry letters* **2015**, *6* (18), 3639-44.
14. Rodríguez-Tinoco, C.; Gonzalez-Silveira, M.; Ràfols-Ribé, J.; Garcia, G.; Rodríguez-Viejo, J., Highly stable glasses of celecoxib: Influence on thermo-kinetic properties, microstructure and response towards crystal growth. *Journal of Non-Crystalline Solids* **2015**, *407*, 256-261.
15. Zhang, K.; Li, Y.; Huang, Q.; Wang, B.; Zheng, X.; Ren, Y.; Yang, W., Ultrastable Amorphous Sb₂Se₃ Film. *The journal of physical chemistry. B* **2017**, *121* (34), 8188-8194.
16. Zhang, A.; Jin, Y.; Liu, T.; Stephens, R. B.; Fakhraai, Z., Polyamorphism of vapor-deposited amorphous selenium in response to light. *Proceedings of the National Academy of Sciences of the United States of America* **2020**, *117* (39), 24076-24081.
17. Yu, H. B.; Luo, Y.; Samwer, K., Ultrastable metallic glass. *Adv Mater* **2013**, *25* (41), 5904-8.
18. Luo, P.; Cao, C. R.; Zhu, F.; Lv, Y. M.; Liu, Y. H.; Wen, P.; Bai, H. Y.; Vaughan, G.; di Michiel, M.; Ruta, B. et al., Ultrastable metallic glasses formed on cold substrates. *Nature communications* **2018**, *9* (1), 1389.
19. Rodriguez-Tinoco, C.; Gonzalez-Silveira, M.; Ramos, M. A.; Rodriguez-Viejo, J., Ultrastable glasses: new perspectives for an old problem. *La Rivista del Nuovo Cimento* **2022**, *45* (5), 325-406.
20. Raegen, A. N.; Yin, J.; Zhou, Q.; Forrest, J. A., Ultrastable monodisperse polymer glass formed by physical vapour deposition. *Nature materials* **2020**, *19* (10), 1110-1113.
21. Yoon, H.; Koh, Y. P.; Simon, S. L.; McKenna, G. B., An Ultrastable Polymeric Glass: Amorphous Fluoropolymer with Extreme Fictive Temperature Reduction by Vacuum Pyrolysis. *Macromolecules* **2017**, *50* (11), 4562-4574.
22. Ramos, S. L.; Oguni, M.; Ishii, K.; Nakayama, H., Character of devitrification, viewed from enthalpic paths, of the vapor-deposited ethylbenzene glasses. *The journal of physical chemistry. B* **2011**, *115* (49), 14327-32.

1
2
3 23. Leon-Gutierrez, E.; Sepulveda, A.; Garcia, G.; Clavaguera-Mora, M. T.; Rodriguez-Viejo, J., Stability of thin film glasses of toluene and ethylbenzene formed by vapor deposition: an in situ nanocalorimetric study. *Physical chemistry chemical physics : PCCP* **2010**, *12* (44), 14693-8.

4 24. Berthier, L.; Charbonneau, P.; Flenner, E.; Zamponi, F., Origin of Ultrastability in Vapor-
5 Deposited Glasses. *Physical review letters* **2017**, *119* (18), 188002.

6 25. Dalal, S. S.; Fakhraai, Z.; Ediger, M. D., High-throughput ellipsometric characterization of
7 vapor-deposited indomethacin glasses. *The journal of physical chemistry. B* **2013**, *117* (49),
8 15415-25.

9 26. Liu, T.; Cheng, K.; Salami-Ranjbaran, E.; Gao, F.; Li, C.; Tong, X.; Lin, Y. C.; Zhang, Y.;
10 Zhang, W.; Klinge, L. et al., The effect of chemical structure on the stability of physical vapor
11 deposited glasses of 1,3,5-triarylbenzene. *The Journal of chemical physics* **2015**, *143* (8), 084506.

12 27. Jin, Y.; Zhang, A.; Wolf, S. E.; Govind, S.; Moore, A. R.; Zhernenkov, M.; Freychet, G.;
13 Arabi Shamsabadi, A.; Fakhraai, Z., Glasses denser than the supercooled liquid. *Proceedings of
14 the National Academy of Sciences of the United States of America* **2021**, *118* (31).

15 28. Fullerton, C. J.; Berthier, L., Density controls the kinetic stability of ultrastable glasses.
16 *EPL (Europhysics Letters)* **2017**, *119* (3).

17 29. Gabriel, J. P.; Riechers, B.; Thoms, E.; Guiseppi-Elie, A.; Ediger, M. D.; Richert, R.,
18 Polyamorphism in vapor-deposited 2-methyltetrahydrofuran: A broadband dielectric relaxation
19 study. *The Journal of chemical physics* **2021**, *154* (2), 024502.

20 30. Yu, H. B.; Tylinski, M.; Guiseppi-Elie, A.; Ediger, M. D.; Richert, R., Suppression of beta
21 Relaxation in Vapor-Deposited Ultrastable Glasses. *Physical review letters* **2015**, *115* (18),
22 185501.

23 31. Rodriguez-Tinoco, C.; Ngai, K. L.; Rams-Baron, M.; Rodriguez-Viejo, J.; Paluch, M.,
24 Distinguishing different classes of secondary relaxations from vapour deposited ultrastable
25 glasses. *Physical chemistry chemical physics : PCCP* **2018**, *20* (34), 21925-21933.

26 32. Kasting, B. J.; Beasley, M. S.; Guiseppi-Elie, A.; Richert, R.; Ediger, M. D., Relationship
27 between aged and vapor-deposited organic glasses: Secondary relaxations in methyl-m-toluate.
28 *The Journal of chemical physics* **2019**, *151* (14), 144502.

29 33. Yokoyama, D.; Adachi, C., In situ real-time spectroscopic ellipsometry measurement for
30 the investigation of molecular orientation in organic amorphous multilayer structures. *Journal of
31 Applied Physics* **2010**, *107* (12), 123512.

32 34. Wolf, S. E.; Fulco, S.; Zhang, A.; Zhao, H.; Walsh, P. J.; Turner, K. T.; Fakhraai, Z., Role
33 of Molecular Layering in the Enhanced Mechanical Properties of Stable Glasses. *The journal of
34 physical chemistry letters* **2022**, *13* (15), 3360-3368.

35 35. Walters, D. M.; Antony, L.; de Pablo, J. J.; Ediger, M. D., Influence of Molecular Shape
36 on the Thermal Stability and Molecular Orientation of Vapor-Deposited Organic Semiconductors.
37 *The journal of physical chemistry letters* **2017**, *8* (14), 3380-3386.

38 36. Yokoyama, D.; Setoguchi, Y.; Sakaguchi, A.; Suzuki, M.; Adachi, C., Orientation Control
39 of Linear-Shaped Molecules in Vacuum-Deposited Organic Amorphous Films and Its Effect on
40 Carrier Mobilities. *Advanced Functional Materials* **2010**, *20* (3), 386-391.

41 37. Whitaker, K. R.; Scifo, D. J.; Ediger, M. D.; Ahrenberg, M.; Schick, C., Highly stable
42 glasses of cis-decalin and cis/trans-decalin mixtures. *The journal of physical chemistry. B* **2013**,
43 *117* (42), 12724-33.

44 38. Jiang, J.; Walters, D. M.; Zhou, D.; Ediger, M. D., Substrate temperature controls
45 molecular orientation in two-component vapor-deposited glasses. *Soft matter* **2016**, *12* (13), 3265-
46 70.

47
48
49
50
51
52
53
54
55
56
57
58
59
60

1
2
3 39. Qiu, Y.; Antony, L. W.; Torkelson, J. M.; de Pablo, J. J.; Ediger, M. D., Tenfold increase
4 in the photostability of an azobenzene guest in vapor-deposited glass mixtures. *The Journal of*
5 *chemical physics* **2018**, *149* (20), 204503.

6 40. Zeng, X.-Y.; Tang, Y.-Q.; Cai, X.-Y.; Tang, J.-X.; Li, Y.-Q., Solution-processed OLEDs
7 for printing displays. *Materials Chemistry Frontiers* **2023**, *7* (7), 1166-1196.

8 41. Tenopala-Carmona, F.; Lee, O. S.; Crovini, E.; Neferu, A. M.; Murawski, C.; Olivier, Y.;
9 Zysman-Colman, E.; Gather, M. C., Identification of the Key Parameters for Horizontal Transition
10 Dipole Orientation in Fluorescent and TADF Organic Light-Emitting Diodes. *Adv Mater* **2021**, *33*
11 (37), e2100677.

12 42. Rafols-Ribe, J.; Will, P. A.; Hanisch, C.; Gonzalez-Silveira, M.; Lenk, S.; Rodriguez-
13 Viejo, J.; Reineke, S., High-performance organic light-emitting diodes comprising ultrastable
14 glass layers. *Sci Adv* **2018**, *4* (5), eaar8332.

15 43. Pakhomenko, E.; He, S.; Holmes, R. J., Polarization-Induced Exciton–Polaron Quenching
16 in Organic Light-Emitting Devices and Its Control by Dipolar Doping. *Advanced Optical*
17 *Materials* **2022**, *10* (23).

18 44. Ediger, M. D., Perspective: Highly stable vapor-deposited glasses. *The Journal of chemical*
19 *physics* **2017**, *147* (21), 210901.

20 45. Haji-Akbari, A.; Debenedetti, P. G., The effect of substrate on thermodynamic and kinetic
21 anisotropies in atomic thin films. *The Journal of chemical physics* **2014**, *141* (2), 024506.

22 46. Haji-Akbari, A.; Debenedetti, P. G., Thermodynamic and kinetic anisotropies in octane
23 thin films. *The Journal of chemical physics* **2015**, *143* (21), 214501.

24 47. Samanta, S.; Huang, G.; Gao, G.; Zhang, Y.; Zhang, A.; Wolf, S.; Woods, C. N.; Jin, Y.;
25 Walsh, P. J.; Fakhraai, Z., Exploring the Importance of Surface Diffusion in Stability of Vapor-
26 Deposited Organic Glasses. *The journal of physical chemistry. B* **2019**, *123* (18), 4108-4117.

27 48. Włodarczyk, P.; Czarnota, B.; Paluch, M.; Pawlus, S.; Ziolo, J., Microscopic origin of
28 secondary modes observed in decahydroisoquinoline. *Journal of Molecular Structure* **2010**, *975*
29 (1-3), 200-204.

30 49. Thoms, E.; Gabriel, J. P.; Guiseppi-Elie, A.; Ediger, M. D.; Richert, R., In situ observation
31 of fast surface dynamics during the vapor-deposition of a stable organic glass. *Soft matter* **2020**,
32 *16* (48), 10860-10864.

33 50. Chen, Z.; Zhao, Y.; Wang, L. M., Enthalpy and dielectric relaxations in supercooled methyl
34 m-toluate. *The Journal of chemical physics* **2009**, *130* (20), 204515.

35 51. Wang, L.-M.; Velikov, V.; Angell, C. A., Direct determination of kinetic fragility indices
36 of glassforming liquids by differential scanning calorimetry: Kinetic versus thermodynamic
37 fragilities. *The Journal of chemical physics* **2002**, *117* (22), 10184-10192.

38 52. Riechers, B.; Guiseppi-Elie, A.; Ediger, M. D.; Richert, R., Ultrastable and polyamorphic
39 states of vapor-deposited 2-methyltetrahydrofuran. *The Journal of chemical physics* **2019**, *150*
40 (21), 214502.

41 53. Dalal, S. S.; Walters, D. M.; Lyubimov, I.; de Pablo, J. J.; Ediger, M. D., Tunable molecular
42 orientation and elevated thermal stability of vapor-deposited organic semiconductors. *Proceedings*
43 *of the National Academy of Sciences of the United States of America* **2015**, *112* (14), 4227-32.

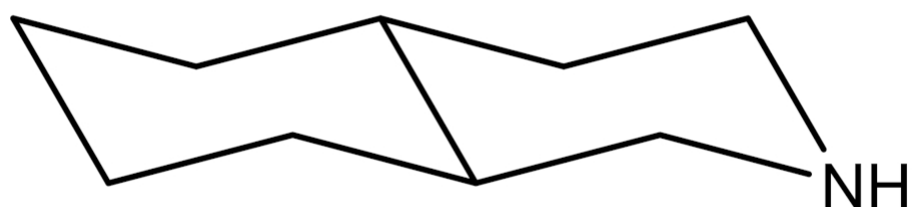
44 54. Ahrenberg, M.; Chua, Y. Z.; Whitaker, K. R.; Huth, H.; Ediger, M. D.; Schick, C., In situ
45 investigation of vapor-deposited glasses of toluene and ethylbenzene via alternating current chip-
46 nanocalorimetry. *The Journal of chemical physics* **2013**, *138* (2), 024501.

47 55. Rafols-Ribe, J.; Gonzalez-Silveira, M.; Rodriguez-Tinoco, C.; Rodriguez-Viejo, J., The
48 role of thermodynamic stability in the characteristics of the devitrification front of vapour-
49

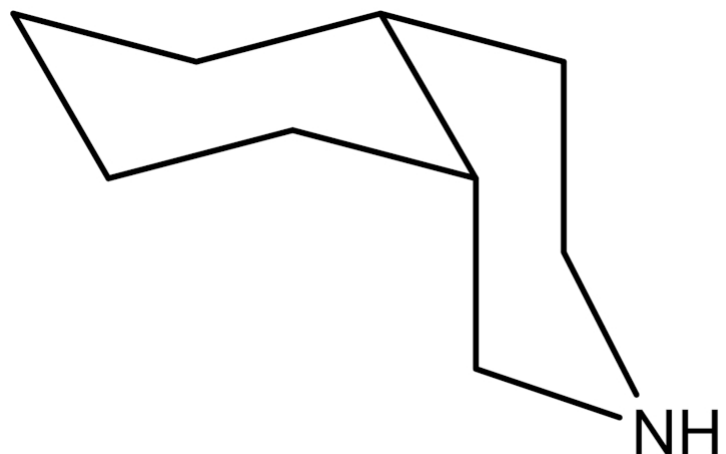
1
2
3 deposited glasses of toluene. *Physical chemistry chemical physics : PCCP* **2017**, *19* (18), 11089-
4 11097.
5 56. Vila-Costa, A.; Rafols-Ribe, J.; Gonzalez-Silveira, M.; Lopeandia, A. F.; Abad-Munoz, L.;
6 Rodriguez-Viejo, J., Nucleation and Growth of the Supercooled Liquid Phase Control Glass
7 Transition in Bulk Ultrastable Glasses. *Physical review letters* **2020**, *124* (7), 076002.
8 57. Kearns, K. L.; Ediger, M. D.; Huth, H.; Schick, C., One Micrometer Length Scale Controls
9 Kinetic Stability of Low-Energy Glasses. *The Journal of Physical Chemistry Letters* **2009**, *1* (1),
10 388-392.
11 58. Swallen, S. F.; Traynor, K.; McMahon, R. J.; Ediger, M. D.; Mates, T. E., Stable glass
12 transformation to supercooled liquid via surface-initiated growth front. *Physical review letters*
13 **2009**, *102* (6), 065503.
14 59. Flenner, E.; Berthier, L.; Charbonneau, P.; Fullerton, C. J., Front-Mediated Melting of
15 Isotropic Ultrastable Glasses. *Physical review letters* **2019**, *123* (17), 175501.
16 60. Wolynes, P. G., Spatiotemporal structures in aging and rejuvenating glasses. *Proceedings
17 of the National Academy of Sciences of the United States of America* **2009**, *106* (5), 1353-8.
18 61. Wisitsorasak, A.; Wolynes, P. G., Fluctuating mobility generation and transport in glasses.
19 *Physical review. E, Statistical, nonlinear, and soft matter physics* **2013**, *88* (2), 022308.
20 62. Leonard, S.; Harrowell, P., Macroscopic facilitation of glassy relaxation kinetics:
21 ultrastable glass films with frontlike thermal response. *The Journal of chemical physics* **2010**, *133*
22 (24), 244502.
23 63. Cubeta, U. S.; Sadtchenko, V., Glass softening kinetics in the limit of high heating rates.
24 *The Journal of chemical physics* **2019**, *150* (9), 094508.
25 64. Sepulveda, A.; Tylinski, M.; Guiseppi-Elie, A.; Richert, R.; Ediger, M. D., Role of fragility
26 in the formation of highly stable organic glasses. *Physical review letters* **2014**, *113* (4), 045901.
27 65. Tylinski, M.; Sepulveda, A.; Walters, D. M.; Chua, Y. Z.; Schick, C.; Ediger, M. D., Vapor-
28 deposited glasses of methyl-m-toluate: How uniform is stable glass transformation? *The Journal
29 of chemical physics* **2015**, *143* (24), 244509.
30 66. Whitaker, K. R.; Tylinski, M.; Ahrenberg, M.; Schick, C.; Ediger, M. D., Kinetic stability
31 and heat capacity of vapor-deposited glasses of o-terphenyl. *The Journal of chemical physics* **2015**,
32 *143* (8), 084511.
33 67. Richert, R.; Duvvuri, K.; Duong, L.-T., Dynamics of glass-forming liquids. VII. Dielectric
34 relaxation of supercooled tris-naphthylbenzene, squalane, and decahydroisoquinoline. *The Journal
35 of chemical physics* **2003**, *118* (4), 1828-1836.
36 68. Paluch, M.; Pawlus, S.; Hensel-Bielowka, S.; Kaminska, E.; Prevosto, D.; Capaccioli, S.;
37 Rolla, P. A.; Ngai, K. L., Two secondary modes in decahydroisoquinoline: which one is the true
38 Johari Goldstein process? *The Journal of chemical physics* **2005**, *122* (23), 234506.
39 69. Rodriguez-Tinoco, C.; Gonzalez-Silveira, M.; Rafols-Ribe, J.; Vila-Costa, A.; Martinez-
40 Garcia, J. C.; Rodriguez-Viejo, J., Surface-Bulk Interplay in Vapor-Deposited Glasses: Crossover
41 Length and the Origin of Front Transformation. *Phys Rev Lett* **2019**, *123* (15), 155501.
42 70. Dalal, S. S.; Ediger, M. D., Influence of substrate temperature on the transformation front
43 velocities that determine thermal stability of vapor-deposited glasses. *The journal of physical
44 chemistry. B* **2015**, *119* (9), 3875-82.
45 71. Whitaker, K. R.; Ahrenberg, M.; Schick, C.; Ediger, M. D., Vapor-deposited
46 alpha,alpha,beta-tris-naphthylbenzene glasses with low heat capacity and high kinetic stability. *J
47 Chem Phys* **2012**, *137* (15), 154502.
48
49
50
51
52
53
54
55
56
57
58
59
60

1
2
3 72. Herrero, C.; Scalliet, C.; Ediger, M. D.; Berthier, L., Two-step devitrification of ultrastable
4 glasses. *Proceedings of the National Academy of Sciences of the United States of America* **2023**,
5 *120* (16), e2220824120.
6
7 73. Sepulveda, A.; Swallen, S. F.; Ediger, M. D., Manipulating the properties of stable organic
8 glasses using kinetic facilitation. *The Journal of chemical physics* **2013**, *138* (12), 12A517.
9
10 74. Jack, R. L.; Berthier, L., The melting of stable glasses is governed by nucleation-and-
11 growth dynamics. *The Journal of chemical physics* **2016**, *144* (24), 244506.
12
13
14
15
16
17
18
19
20
21
22
23
24
25
26
27
28
29
30
31
32
33
34
35
36
37
38
39
40
41
42
43
44
45
46
47
48
49
50
51
52
53
54
55
56
57
58
59
60

trans-DHIQ



cis-DHIQ

Figure 1. Structures of trans-DHIQ and cis-DHIQ (C₉H₁₇N), T_g ≈ 180 K.

84x84mm (300 x 300 DPI)

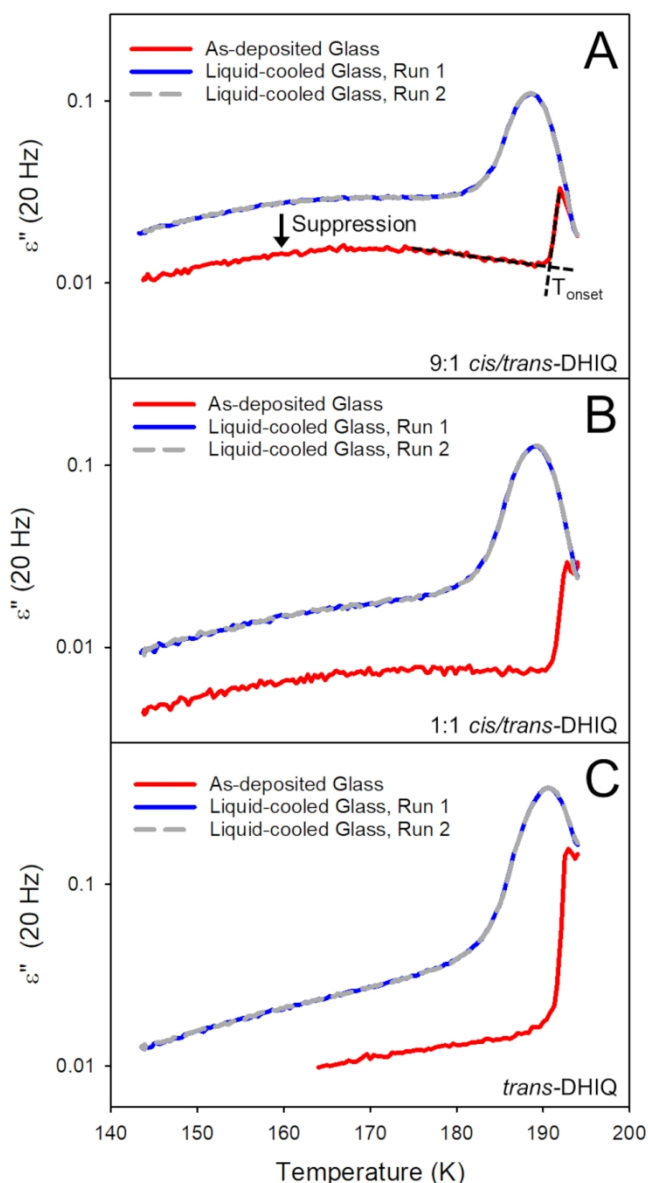


Figure 2. Dielectric loss at 20 Hz as a function of temperature for kinetically stable vapor-deposited DHIQ mixtures. A) 9:1 cis/trans-DHIQ ($T_{dep} = 160$ K), B) 1:1 cis/trans DHIQ ($T_{dep} = 160$ K), C) 100% trans-DHIQ ($T_{dep} = 158$ K). In all three cases the as-deposited glasses display enhanced kinetic stability and secondary relaxation suppression relative to the liquid-cooled glass (runs 1 and 2). Heating and cooling rates were 5 K/min. Film thickness ≈ 700 nm.

84x155mm (300 x 300 DPI)

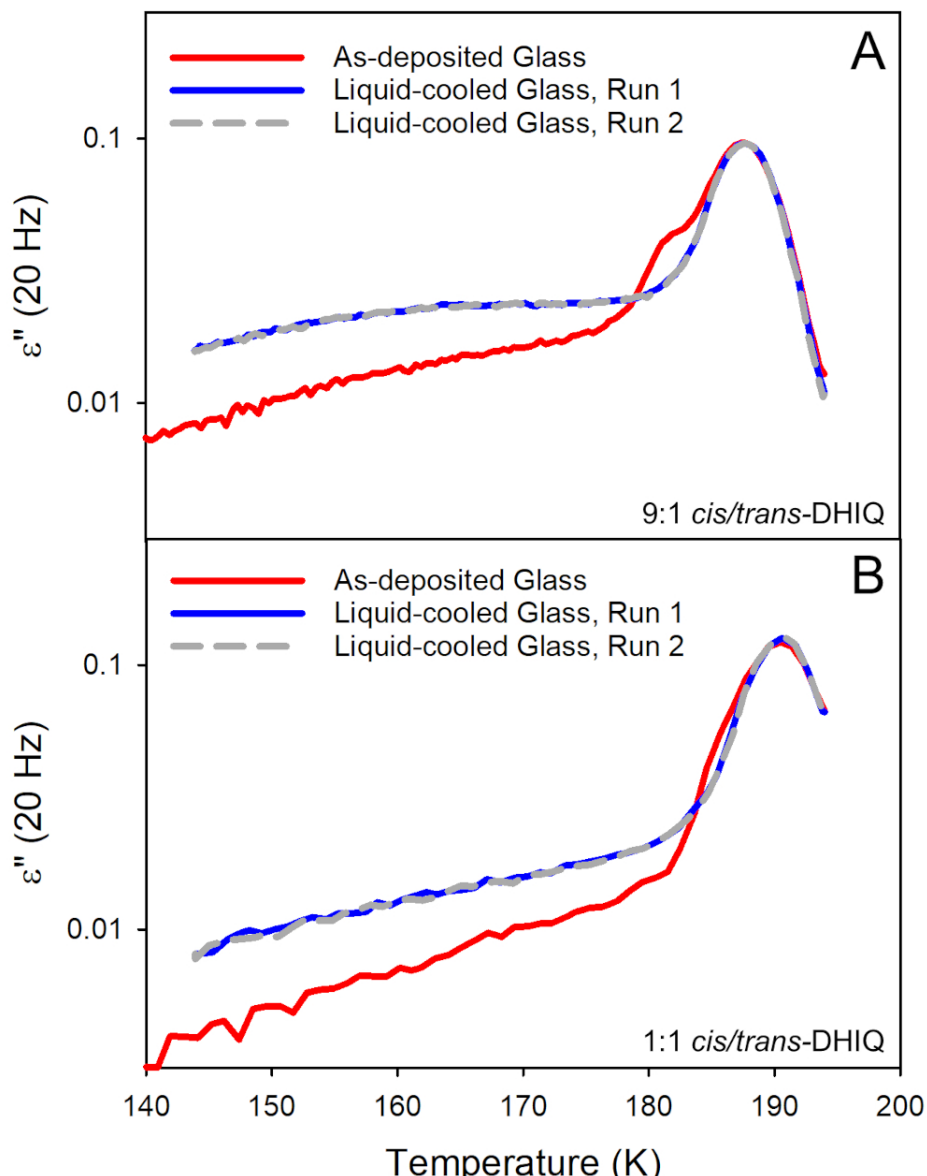


Figure 3. Dielectric loss at 20 Hz as a function of temperature for kinetically unstable vapor-deposited DHIQ mixtures prepared at temperatures near $0.75T_g$. A) 9:1 *cis/trans*-DHIQ ($T_{dep} = 130 \text{ K}$, B) 1:1 *cis/trans*-DHIQ ($T_{dep} = 131 \text{ K}$). In both cases, the as-deposited glass displays a sharp increase in loss amplitude at a lower temperature than the liquid-cooled glass (runs 1 and 2). Heating and cooling rates were 5 K/min. Film thickness $\approx 700 \text{ nm}$.

84x108mm (300 x 300 DPI)

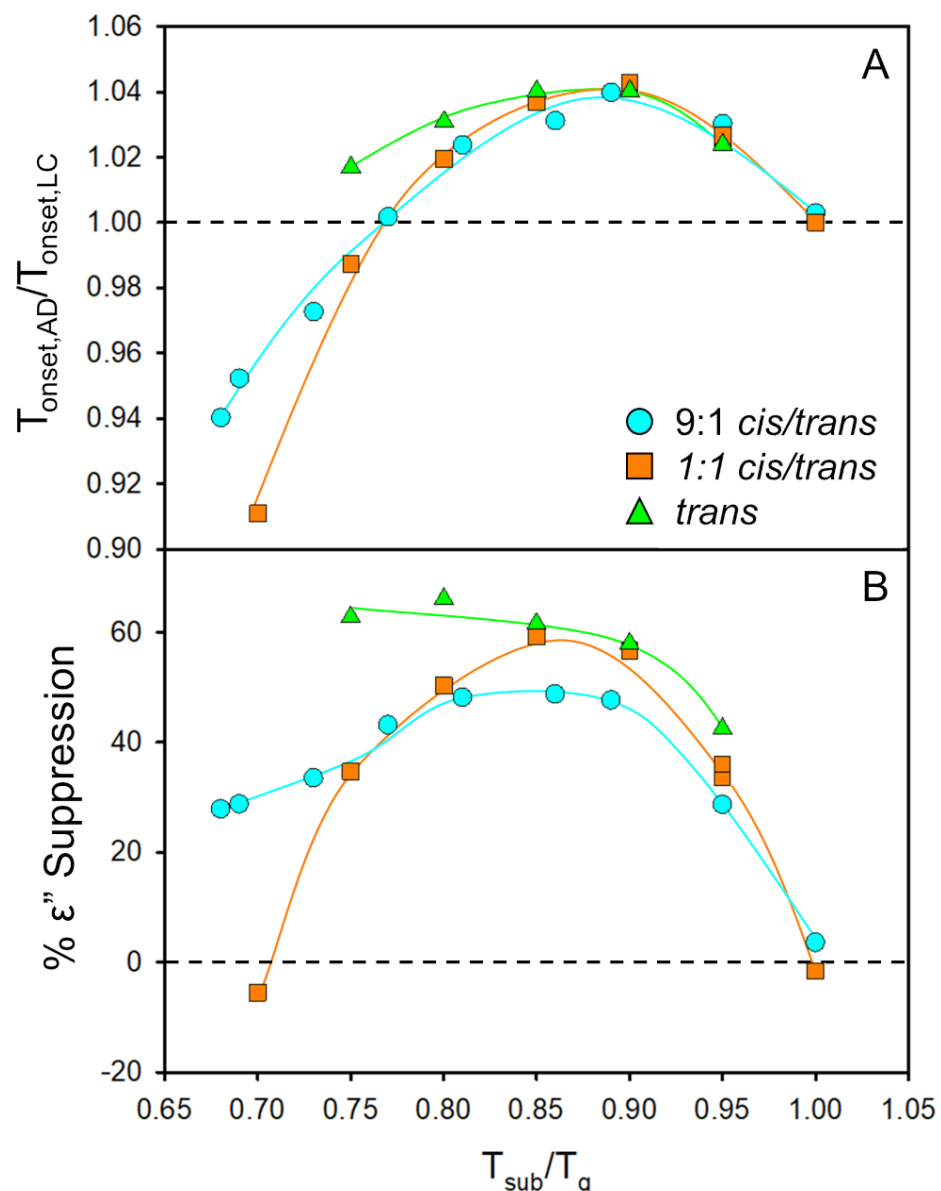


Figure 4. Kinetic stability (A) and suppression of secondary relaxations (B) for vapor-deposited DHIQ glasses as a function of substrate temperature scaled by T_g . $T_{\text{onset,AD}}/T_{\text{onset,LC}}$ is the ratio of the onset temperatures obtained using the tangent method for the as-deposited and liquid-cooled glasses respectively. The y-axis was calculated from the ratio of the 20 Hz loss amplitude of the as-deposited glass to the liquid-cooled glass at $T_g - 10$ K. Lines are a guide to the eye.

84x107mm (300 x 300 DPI)

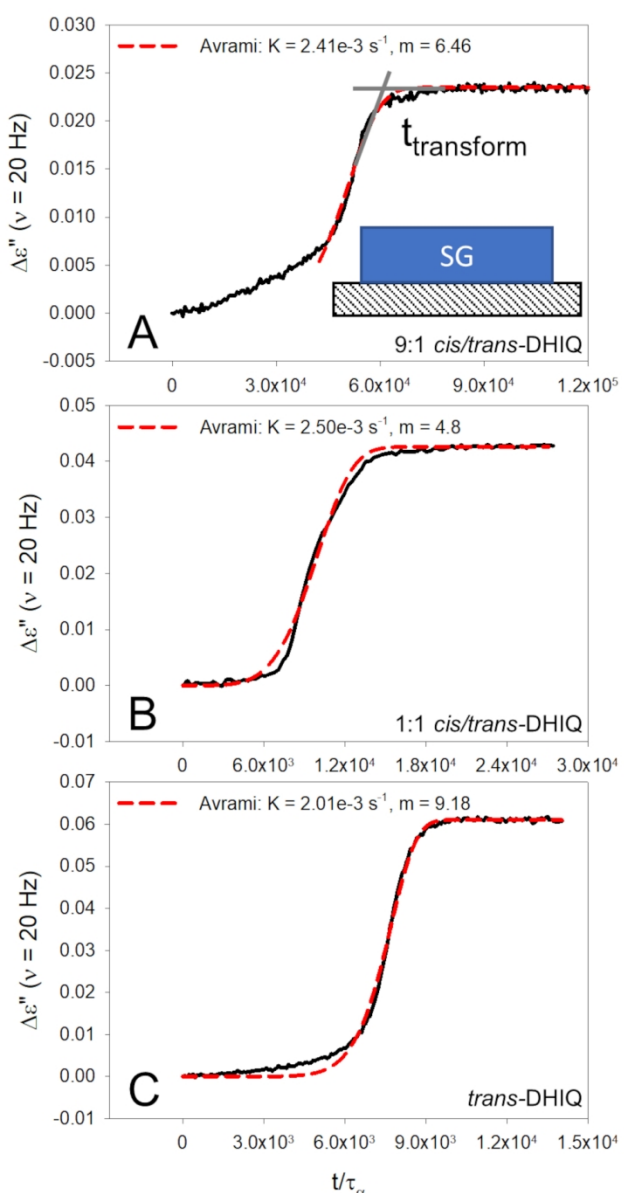


Figure 5. Isothermal annealing experiments for single layer vapor-deposited glasses of isomeric mixtures of DHIQ. A) 9:1 cis/trans, B) 1:1 cis/trans, C) pure trans-DHIQ. The vertical axis is the change in the dielectric signal at 20 Hz since reaching the annealing temperature. The horizontal axis is the time since reaching the annealing temperature scaled by the τ_α of the supercooled liquid (measured after the transformation had completed). Transformation curves were fit to an unconstrained Avrami model with the resulting parameters listed in the respective panels. The amount of the curve that the fit covers represents the range of data used in the fit. Films were all approximately 750 nm thick. Panel A inset: schematic of layer geometry with a stable glass (SG) on top of the interdigitated electrode device. Tanneal = 185 K, 184 K, and 184 K for each panel respectively. Tdep = 160 K, 160 K, and 158 K for each panel respectively.

84x161mm (300 x 300 DPI)

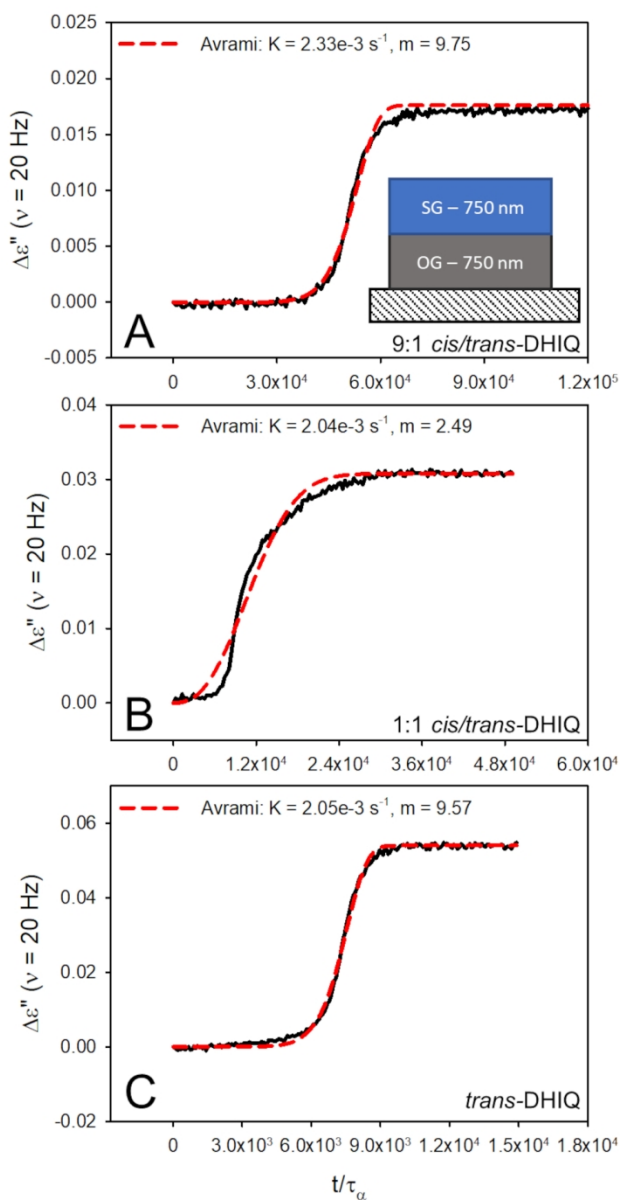


Figure 6. Isothermal annealing experiments for vapor-deposited glasses of isomeric mixtures of DHIQ deposited on top of an ordinary glass of the same material. A) 9:1 cis/trans, B) 1:1 cis/trans, C) pure trans-DHIQ. Stable films were all approximately 750 nm thick bringing the total film thickness to 1.5 μ m. The meaning of the axes is the same as in Figure 5. Top panel inset: schematic of layer geometry with a stable glass (SG) on top of an ordinary glass (OG). Anneal = 185 K, 184 K, and 184 K for each panel respectively. T_{dep} = 160 K, 160 K, and 158 K for each panel respectively.

84x161mm (300 x 300 DPI)

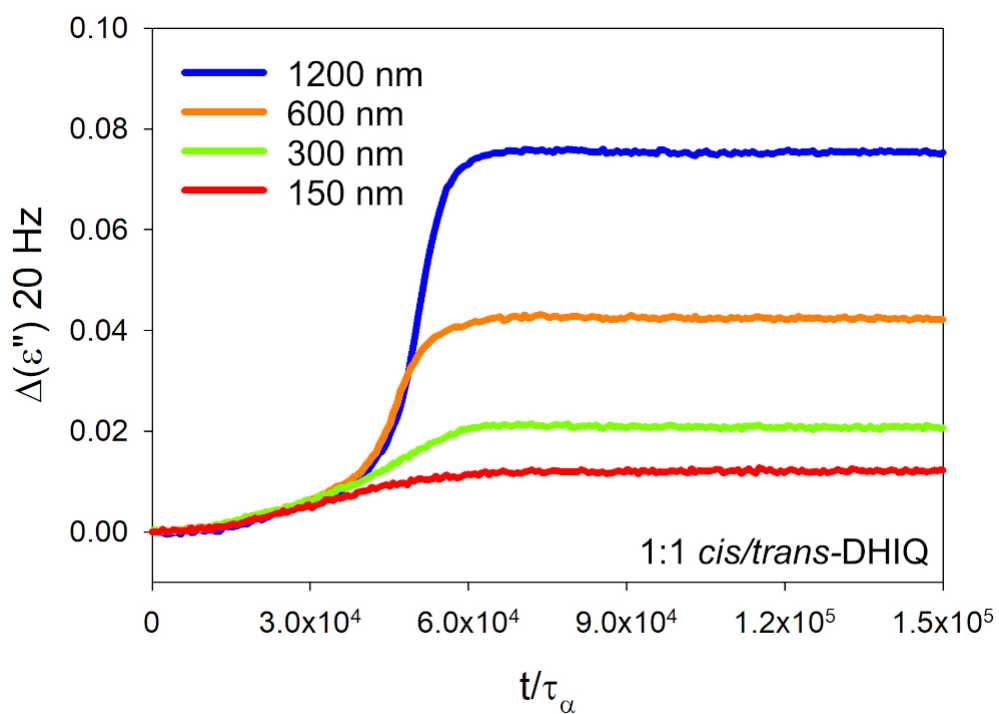
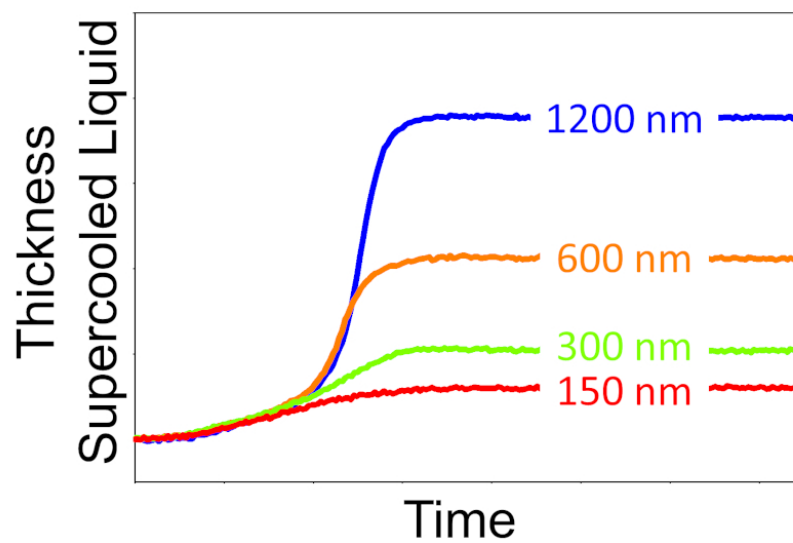


Figure 7. Isothermal annealing experiments for vapor-deposited glasses of 1:1 cis/trans-DHIQ of various thicknesses, Tanneal = 186 K Tdep = 155 K. The meaning of the axes is the same as Figures 5 and 6.

84x60mm (300 x 300 DPI)



TOC Graphic

82x44mm (300 x 300 DPI)